Supplementary Material Available: Rate data for proton and deuteron transfer (Table I) and amine-catalyzed deprotonation and dedeuteriation (Table III) of 1,3-Me_2-5-*t*-Bu(BA) for proton and deuteron transfer in 5-*t*-Bu(BA) (Table VI) and for proton transfer in 1,3-*i*-Pr_2(BA) and 1,5-*i*-Pr_2(BA) (Table VIII) are available as are ^{13}C chemical shifts in 5-*t*-Bu(BA) (Table V) (12 pages). Ordering information is given on any current masthead page.

The Crystal and Molecular Structure of Tris(substituted amino) Sulfonium Ions

William B. Farnham,* David A. Dixon,* William J. Middleton, Joseph C. Calabrese, Richard L. Harlow, J. F. Whitney, Glover A. Jones, and Lloyd J. Guggenberger

Contribution No. 4038 from the Central Research and Development Department, E. I. du Pont de Nemours and Company, Inc., Experimental Station, Wilmington, Delaware 19898. *Received May 14, 1986*

Abstract: The synthesis and crystal structures determined by X-ray diffraction techniques for a number of salts of the tris(dimethylamino)sulfonium cation (methyl-TAS) are reported. The structures of the methyl-TAS cation are all very similar, and the cation possesses approximate C_s symmetry with two equivalent $(CH_3)_2N''$ groups and one unique $(CH_3)_2N'$ group. The structure is characterized by a long S–N′ bond distance of 1.689 Å and two short S–N″ bond distances of 1.615 Å. The N″–S–N″ bond angle is large, 115.4°, while the two N′–S–N″ bond angles are smaller, 99.2°, similar to those in other sulfonium ions. The unique amino group is pyramidal, and the equivalent amino groups are approximately planar. The results suggest multibonding character in the S–N″ bonds. Ab initio molecular orbital calculations on $S(NH_2)_3^+$ with a large basis set confirm the observed X-ray crystal structure. A detailed conformational analysis of the surface for inversion at S^+ is presented. Analytically calculated infrared frequencies and intensities are presented, and these results are consistent with the observed structures. The sulfur is found to be quite positive, $q(S) = 0.92e$. The crystal structure of a tricyclic TAS derivative is also presented. Ring strain causes deviations from the preferred structure found for methyl-TAS. A very short nominally nonbonded S–O distance of 2.55 Å is observed.

Tris(dialkylamino)sulfonium cations, $(R_2N)_3S^+$,[1] are unique in their ability to form stable, isolable salts containing a variety of unusual anions. Among these anions are difluorotrialkylsiliconates,[2] perfluorinated alkoxides,[3] perfluorinated carbanions,[4] and hypervalent iodinanides.[5] The convenient chemical and physical properties of several of these species have led to structural determinations, studies of dynamic properties in solution, and a variety of new synthetic methods.[6] TAS salts were also important in early studies which led to the group transfer polymerization process.[7]

We have characterized the structures of six tris(dimethylamino)sulfonium (methyl-TAS) salts: methyl-TAS + I^- (**1**), methyl-TAS + Br^- (**2**), methyl-TAS + FHF^- (**3**), methyl-TAS + CF_3O^- (**4**), methyl-TAS + 5′ (**5**), and methyl-TAS + 6′ (**6**).

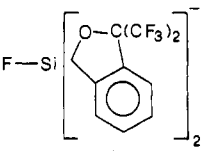

5′

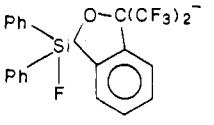

6′

The structure of the salt **8** of 5′ with another TAS derivative **7**, has also been studied. The structures of **4**[3] and **5**[8] have been reported by us previously with the focus on the structures of the anions.

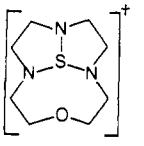

7

We have also calculated the structure of $(R_2N)_3S^+$ for R = H (**9**) by using ab initio molecular orbital theory with a large basis set. The calculations provide more information about the electronic structure and conformational properties of this novel ion and provide insight into the ion's unusual bonding.

Experimental Section

Synthesis. General Remarks. Proton and fluorine chemical shifts are reported in ppm downfield from tetramethylsilane and $CFCl_3$, respectively. ^1H NMR spectra were recorded on a Nicolet NT WB-360

(1) We have chosen the acronym TAS (tris amino sulfonium) to represent this class of cations.

(2) (a) Middleton, W. J. U.S. Patent 3940402, Feb 1976. (b) Middleton, W. J. *Org. Synth.* **1985**, *64*, 221.

(3) Farnham, W. B.; Smart, B. E.; Middleton, W. J.; Calabrese, J. C.; Dixon, D. A. *J. Am. Chem. Soc.* **1985**, *107*, 4565.

(4) (a) Smart, B. E.; Middleton, W. J.; Farnham, W. B. *J. Am. Chem. Soc.* **1986**, *108*, 4905. (b) Farnham, W. B.; Middleton, W. J.; Fultz, W. C.; Smart, B. E. *J. Am. Chem. Soc.* **1986**, *108*, 3125.

(5) Farnham, W. B.; Calabrese, J. C. *J. Am. Chem. Soc.* **1986**, *108*, 2449.

(6) Much of the synthetic work features TAS difluorotrialkylsiliconates as potent, anhydrous sources of fluoride. See, for example: (a) Noyori, R.; Nishida, I.; Sakata, J. *Tetrahedron Lett.* **1980**, 2085. (b) Noyori, R.; Nishida, I.; Sakata, J.; Nishizawa, M. *J. Am. Chem. Soc.* **1980**, *102*, 1223. (c) Noyori, R.; Nishida, I.; Sakata, J. *J. Am. Chem. Soc.* **1981**, *103*, 2108. (d) RajanBabu, T. V. *J. Org. Chem.* **1984**, *49*, 2083. (e) RajanBabu, T. V.; Fukunaga, T. *J. Org. Chem.* **1984**, *49*, 4571. (f) RajanBabu, T. V.; Reddy, G. S.; Fukunaga, T. *J. Am. Chem. Soc.* **1985**, *107*, 5473. (g) Fujita, M.; Hiyama, T. *J. Am. Chem. Soc.* **1985**, *107*, 4085. (h) Card, P. J.; Hitz, W. D. *J. Am. Chem. Soc.* **1984**, *106*, 5348. (i) Trainor, G. C. *J. Carbohydr. Chem.* **1985**, *4*, 545. (j) Fujita, M.; Hiyama, T. *J. Am. Chem. Soc.* **1985**, *107*, 8294.

(7) Webster, O. W.; Hertler, W. R.; Sogah, D. Y.; Farnham, W. B.; RajanBabu, T. V. *J. Am. Chem. Soc.* **1983**, *105*, 5706. Webster, O. W. U.S. Patent 4417034, Nov 1983.

(8) Farnham, W. B.; Harlow, R. L. *J. Am. Chem. Soc.* **1981**, *103*, 4608.

0002-7863/87/1509-0476$01.50/0

Table I. Crystal Data

property	1	2	3	6	8
molecular formula	$((CH_3)_2N)_3S^+ \cdot I^-$ [a]	$((CH_3)_2N)_3S^+Br^- \cdot {}^1/_2H_2O$	$((CH_3)_2N)_3S^+ \cdot FHF^-$	$((CH_3)_2N)_3S^+ \cdot C_{21}H_{14}F_7OSi^-$	$S^+N_3C_8H_{16}O \cdot C_{18}H_8F_{13}O_2Si^-$
molecular wt g/mol	291.20	253.2	203.303	607.727	733.65
crystal system	orthorhombic	monoclinic	triclinic	triclinic	triclinic
space group	*Pbam* (no. 55)	*P2/c*	*P*$\bar{1}$	*P*$\bar{1}$	*P*$\bar{1}$
a (Å)	12.468 (1)	14.475 (6)	7.311 (1)	10.218 (4)	8.842 (3)
b (Å)	16.482 (1)	7.059 (8)	12.045 (2)	15.441 (7)	19.011 (5)
c (Å)	11.351 (1)	12.028 (6)	6.097 (1)	9.741 (4)	8.621 (3)
α			90.83 (1)	106.14 (3)	94.60 (2)
β			102.01 (1)	107.57 (3)	90.55 (3)
γ			83.39 (1)	87.17 (4)	83.64 (3)
Z	8	4	2	2	2
V (A^3)	2332.6	1167.7	521.6	1406.45	733.65
p (g cm^{-3}) calcd	1.658	1.44	1.294	1.435	1.697
absrptn coeff (cm^{-1})	28.45	38.6	2.85	2.219	2.655
crystal size (mm)	0.20 × 0.19 × 0.40	0.60 × 0.50 × 0.18	0.25 × 0.15 × 0.40	0.19 × 0.06 × 0.35	0.25 × 0.15 × 0.35
no. of reflctns	2922	1533	2393	6233	6588
no. of reflctns $I > 2\sigma(I)$	2162[b]	1272[c]	1955	3987	4551
no. of variables	181	171	185	489	496
R	0.021	0.054	0.034	0.048	0.043
R_w	0.025	0.060	0.036	0.052	0.041

[a] Two independent ion pairs, both using crystallographic mirror symmetry. [b] $3\sigma(I)$. [c] $2\sigma(F_o)$.

spectrometer. ^{19}F NMR spectra were recorded on a Nicolet NT-200 spectrometer at 188.2 MHz.

Solvents and Reagents. Tetrahydrofuran and dioxane were distilled from sodium/benzophenone and stored over activated 4-Å molecular sieves. Reactions were carried out in an atmosphere of dry nitrogen or argon. Although special handling procedures were not always required, manipulations of many of the salts were routinely performed in a Vacuum Atmospheres drybox.

Preparation and Characterization of Tris(dimethylamino)sulfonium Bromide (2). A solution of tris(dimethylamino)sulfonium difluorotrimethylsiliconate (27.4 g, 0.10 mol) in acetonitrile (30 mL) at 0 °C was treated dropwise with allyl bromide (29.3 g, 0.24 mol). The mixture was stirred for 18 h at ambient temperature. Filtration after addition of ether gave a white solid (13.8 g). Recrystallization from dichloromethane/ether gave a sample with mp 176–177 °C dec. Anal. C, H, N, S, Br.

Preparation of 3. The preparation and characterization details have been published.[7]

Preparation of 4. Preparation and characterization details have been published.[3] The variable temperature ^1H NMR data were obtained as follows. The width at half-height of the methyl group signal was monitored as a function of temperature at 360 MHz by using a solution of **4** in CD_2Cl_2 with C_6H_6 as a line shape reference. The methyl singlet broadened only slightly at −90 °C ($\omega_{1/2}$ = 2.0 Hz) by comparison with the spectrum recorded at +25 °C ($\omega_{1/2}$ = 0.9 Hz).

Preparation and Characterization of 5. Preparation and characterization of TAS fluorosiliconate **5** have been published.[8]

1,1-Diphenyl-3,3-bis(trifluoromethyl)-(3*H*)-2,1-benzoxasilole (10). A solution of hexafluorocumyl alcohol (48.8 g, 0.2 mol) and tetramethylethylenediamine (30 mL) in petroleum ether (400 mL) was treated with butyllithium (0.4 mol) in hexane. After addition was complete, the mixture was heated at 40 °C for 15 h. Diphenyldichlorosilane (50.6 g, 0.2 mol) in petroleum ether (100 mL) was added dropwise at −50 °C, and the mixture was warmed to 25 °C. Ether (250 mL) was added, and the mixture was heated to reflux for 2.0 h. The reaction mixture was cooled to 0 °C, treated with water, and diluted with ether. The organic layer was washed with water and saturated sodium chloride and dried ($MgSO_4$). Evaporation gave a residue which was Kugelrohr distilled to provide a fraction with bp ca. 130–150 °C (0.2 mmHg). Recrystallization from hexane gave 19.0 g of white solid, mp 85–87 °C: ^1H NMR ($CDCl_3$) 8.1–7.3 (m); ^{19}F NMR −75.94 (s).

Tris(dimethylamino)sulfonium Fluorosiliconate (6). A solution of the silane **10** (4.95 g, 11.7 mmol) in acetonitrile (20 mL) was treated with tris(dimethylamino)sulfonium trimethyldifluorosiliconate (3.08 g, 11.2 mmol) and stirred for 0.5 h. Half the solvent was removed under a stream of nitrogen. Slow addition of ether led to formation of a white solid which was filtered, washed with ether, and dried to give 6.33 g, mp 117–118 °C: ^1H NMR (CD_3CN) 8.43–8.28 (m, 1 H), 8.17–7.87 (m, 3 H), 7.75–7.20 (m, 10 H), 2.77 (s, 18 H); ^{19}F NMR −107.26 (s, 1 F), −74.11 (s, 6 F). Anal. C, H, N.

1,4,7-Triaza-10-oxacyclododecane (11) was prepared from the tritosylate according to the procedure of Richman and Atkins.[9]

1,4,7-Tris(trimethylsilyl)-1,4,7-triaza-10-oxacyclododecane (12). A solution of triamine **11** (17.3 g, 0.10 mol) in THF (100 mL) at −78 °C was treated with butyllithium (0.30 mol). The resulting mixture was warmed to 10 °C, then cooled to −78 °C, and treated with chlorotrimethylsilane (35.6 g, 0.33 mol). The mixture was warmed to 25 °C, stirred 18 h, filtered under nitrogen, and evaporated. Kugelrohr distillation of the residue provided 32.9 g of colorless oil, bp 120–130°/0.15 mmHg (85%): ^1H NMR ($CDCl_3$) 3.50–2.75 (m, 16 H), 0.05 and 0.04 (two singlets, 27 H).

Preparation and Characterization of the Salt of Methyl-TAS and $Me_3SiF_2^-$ (13). Preparation and characterization data have been published.[2]

Preparation of Sulfonium Salt[8] 14 (X = HF_2, Me_3SiF_2). A solution of tris(trimethylsilyl)oxacyclene **12** (32.8 g, 84 mmol) in ether (275 mL) at −78 °C was treated slowly with sulfur tetrafluoride (9.1 g, 84 mmol). The reaction mixture was warmed to 25 °C over a ca. 33-h period and was stirred for 48 h. A light tan solid was filtered under nitrogen pressure to give 14.7 g of material [^1H NMR (CD_3CN) 4.25–3.20 (m), −0.1 (s), 16.3 (t, $J \sim 120$ Hz)]. Integration revealed a 45/55 mixture of HF_2^-/$Me_3SiF_2^-$ anions. Structure confirmation was carried out by conversion to the more easily handled salt of **7** + **5′**, **8**.

Preparation of Sulfonium Salt 8. A mixture of spirosilane **15**[10] (2.56 g, 5 mmol) and acetonitrile (5 mL) was treated with crude sulfonium salt **14** (1.39 g). After 15 min at 25 °C, the volatiles were removed under

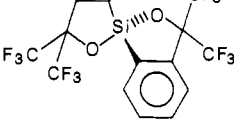

15

vacuum, and the residue was triturated with ether several times and filtered to give 2.85 g of crude **8**. Recrystallization from THF/ether gave 2.35 g of colorless crystals, mp 157–158.5 °C: ^1H NMR (CD_3CN) 8.30–8.05 (m, 2 H), 7.75–7.30 (m, 6 H), 4.10–3.80 (m, 2 H), 3.80–3.10 (m, 14 H); ^{13}C NMR (cation signals only) 51.01, 51.94, 55.31, 70.79. Anal. C, H, N, F, S.

Crystal Structures

The original crystal structure data for **4**[3] and **5**[8] have been published previously. We report here the crystal structure information for the methyl-TAS salts **1–3** and **6** and the salt **8** of **7** with **5′**. The crystal data is reported in Table I.

X-ray Data of 1, 3, 6, and 8. The X-ray data were collected at −100 °C on a Syntex R-3 diffractometer equipped with a graphite monochromator. Mo Kα radiation was used. The data points were collected over the range of $4° \leq 2\theta \leq 55°$. The ω

(9) Richman, J. E.; Atkins, T. J. *J. Am. Chem. Soc.* **1974**, *96*, 2268.

(10) Perozzi, E. F.; Martin, J. C. *J. Am. Chem. Soc.* **1979**, *101*, 1591.

Table II. Bond Lengths (Å) and Angles for Methyl-TAS from the Crystal Structure Data

	1	1′	2	3	4	5	5′	6
r(S–N′)	1.685 (3)	1.695 (3)	1.682 (4)	1.686 (1)	1.689 (3)	1.687 (5)	1.692 (4)	1.693 (3)
r(S–N″)	1.620 (2)	1.618 (2)	1.608 (6)	1.642 (1)	1.619 (2)	1.607 (5)	1.621 (4)	1.606 (3)
r(S–N‴)	1.620 (2)	1.618 (2)	1.608 (6)	1.604 (1)	1.619 (2)	1.609 (5)	1.602 (4)	1.625 (3)
r(N′–C′)	1.475 (4)	1.482 (4)	1.480 (8)	1.482 (2)	1.476 (4)	1.480 (7)	1.500 (7)	1.491 (5)
r(N′–C″)	1.475 (4)	1.482 (4)	1.483 (8)	1.483 (2)	1.476 (4)	1.485 (7)	1.472 (7)	1.475 (5)
r(N″–C″)	1.471 (3)	1.475 (4)	1.474 (10)	1.466 (2)	1.465 (3)	1.479 (6)	1.484 (6)	1.475 (4)
r(N″–C′)	1.477 (3)	1.463 (4)	1.476 (8)	1.478 (2)	1.468 (3)	1.457 (7)	1.451 (7)	1.471 (4)
r(N‴–C″)	1.471 (3)	1.475 (4)	1.448 (9)	1.468 (2)	1.465 (3)	1.477 (7)	1.460 (6)	1.470 (4)
r(N‴–C′)	1.477 (3)	1.463 (4)	1.464 (8)	1.454 (2)	1.468 (3)	1.445 (7)	1.463 (7)	1.474 (4)
θ(SN′C′)	112.4 (2)	111.5 (2)	111.2 (3)	112.2 (2)	111.9 (2)	110.6 (4)	110.6 (4)	110.0 (2)
θ(SN′C″)	112.4 (2)	111.5 (2)	113.1 (4)	110.7 (1)	111.9 (2)	111.0 (4)	110.5 (4)	112.4 (2)
θ(C′N′C″)	110.8 (3)	110.1 (4)	109.8 (4)	110.8 (1)	111.6 (4)	110.5 (5)	111.5 (5)	110.8 (3)
θ(SN″C′)	114.4 (2)	115.4 (2)	113.3 (4)	111.3 (1)	114.8 (2)	114.9 (4)	112.7 (4)	117.2 (3)
θ(SN″C″)	123.2 (2)	123.3 (2)	123.8 (4)	120.6 (1)	123.2 (2)	124.4 (4)	123.1 (4)	124.6 (3)
θ(C′N″C″)	114.9 (2)	114.5 (2)	114.7 (4)	114.0 (2)	115.3 (2)	115.6 (5)	115.3 (4)	117.2 (3)
θ(SN‴C′)	114.4 (2)	115.4 (2)	115.9 (4)	117.9 (1)	114.8 (2)	117.6 (4)	116.6 (4)	114.9 (2)
θ(SN‴C″)	123.2 (2)	123.3 (2)	124.5 (4)	125.1 (1)	123.2 (2)	123.2 (4)	124.6 (4)	124.4 (2)
θ(C′N‴C″)	114.9 (2)	114.5 (2)	115.5 (5)	116.4 (2)	115.3 (2)	116.2 (5)	116.6 (5)	115.9 (3)
θ(N′SN″)	98.6 (1)	99.0 (1)	99.0 (2)	98.3 (1)	98.7 (1)	99.5 (3)	98.9 (2)	101.8 (1)
θ(N′SN‴)	98.6 (1)	99.0 (1)	98.5 (2)	100.7 (1)	98.7 (1)	100.4 (3)	100.5 (3)	98.3 (1)
θ(N″SN‴)	116.6 (2)	116.3 (2)	115.6 (3)	114.4 (1)	116.1 (1)	114.9 (3)	115.0 (3)	113.9 (2)

scan method was employed with a scan width of 1.00° ω and scan speeds of 2.00–9.80°/min. An absorption correction (DIFABS)[11] was applied for **1**. Lorentz and polarization corrections were applied. The structures for **1** and **6** were corrected for a 3% decrease in intensity.

The structure for **1** was solved by automated Patterson analysis (PHASE).[12] The solution was complicated by the uneven distribution of intensities and the weak 001(1 odd) diffraction line due to the special positions of the iodine anions. The other three structures were solved by direct methods (MULTAN).[13] For each of the four X-ray analyses, a full matrix least-squares refinement was carried out. Scattering factors were taken from a standard source[14] and anomalous terms were included for S, I, Si, and F where appropriate. All non-hydrogen atoms were refined anisotropically; all hydrogens were refined isotropically.

X-ray. 2. Data were collected on a Picker four-circle automatic diffractometer. The θ–2θ scan technique was used with Zr-filtered Mo radiation. The data were measured to 45° in 2Θ with a scan range of 1.75° (1°/min) plus the $K\alpha_1$–$K\alpha_2$ separation. The data were corrected for absorption effects and a 1% (in F_0) overall decomposition correction was applied to the data. The structure was solved by Patterson techniques. The Br^- is split between two special positions (0,0,0-symmetry 1 and $^1/_2$, *Y*, 1/4-symmetry 2). A broad peak on an electron density difference map on the 0, *Y*, $^1/_2$ twofold axis was interpreted as an oxygen of a water molecule. Least-squares refinements proceeded with anisotropic temperature factors for all heavy atoms. Hydrogen atoms were included with isotropic temperature factors of 6.0 Å^2 in calculated tetrahedral positions most consistent with the electron density difference map. Water hydrogen atoms were not included.

Theoretical Calculations. The initial calculations on the perhydro derivative of TAS, $S(NH_2)_3^+$ **9** were done with the program HONDO[15] on an IBM 3081. A polarized double zeta basis set of the form (11s7p1d/9s5p1d/4s1p)/[6s4p1d/3s2p1d/2s1p], Basis Set 1, was used with exponents and coefficients from Dunning and Hay[16] (ζ_{3d}(S) = 0.60). The starting coordinates and conformation for **9a** were taken from the crystal structure (C_1 symmetry) for **6** with the CH_3 groups replaced by appropriately positioned hydrogen atoms. The geometry was gradient optimized[17] until no coordinate changed by >0.002 au. Subsequent calculations started from these coordinates and were done with the program GRADSCF on a CRAY-XMP/48 equipped with an SSD. For these calculations, a slightly larger basis set, Basis Set 2, of the form (13s9p1d/9s5p1d/4s1p)/[6s4p1d/4s2p1d/2s1p] was used with exponents and coefficients for the s and p basis for S from McLean and Chandler[19] and for N and H from Dunning.[20] The same exponents as used in Basis Set 1 for the polarization functions were used for Basis Set 2. The geometry was gradient optimized until the maximum change in any coordinate was <0.0005 au. The force field and infrared intensities were determined analytically at the final geometry.

In order to gain more information about the conformational flexibility of $S(NH_2)_3^+$, the additional geometries shown in Figure 1 were optimized with Basis Set 2. The first two structures have pyramidal sulfur atoms, and **9b** has pyramidal nitrogens while in **9c** the nitrogens are planar. The remaining structures involve

Table III. Geometric Parameters for 7[a]

	Bond Distances		
$r(S–N_1)$	1.685 (2)	$r(N_3–C_8)$	1.466 (4)
$r(S–N_2)$	1.704 (2)	$r(C_1–C_2)$	1.515 (4)
$r(S–N_3)$	1.644 (3)	$r(C_3–C_4)$	1.435 (5)
$r(N_1–C_1)$	1.471 (3)	$r(C_5–C_6)$	1.498 (4)
$r(N_1–C_5)$	1.463 (4)	$r(C_6–O)$	1.435 (4)
$r(N_2–C_2)$	1.476 (4)	$r(C_7–O)$	1.422 (4)
$r(N_2–C_3)$	1.466 (5)	$r(C_7–C_8)$	1.508 (4)
$r(N_3–C_4)$	1.416 (4)		
	Bond Angles		
$\theta(N_1SN_2)$	95.1 (1)	$\theta(N_1C_1C_2)$	102.8 (2)
$\theta(N_1SN_3)$	113.0 (1)	$\theta(N_2C_2C_1)$	106.3 (2)
$\theta(N_2SN_3)$	94.6 (1)	$\theta(N_2C_3C_4)$	112.9 (3)
$\theta(SN_1C_1)$	118.0 (2)	$\theta(N_3C_4C_3)$	108.5 (3)
$\theta(SN_1C_5)$	110.2 (2)	$\theta(N_1C_5C_6)$	112.0 (2)
$\theta(C_1N_1C_5)$	115.3 (2)	$\theta(N_3C_8C_7)$	109.6 (2)
$\theta(SN_2C_2)$	107.2 (2)	$\theta(C_5C_6O_3)$	111.5 (2)
$\theta(SN_2C_3)$	108.5 (2)	$\theta(C_8C_7O_3)$	106.7 (2)
$\theta(C_2N_2C_3)$	115.3 (2)	$\theta(C_6O_3C_7)$	116.8 (2)
$\theta(SN_3C_4)$	115.0 (2)		
$\theta(SN_3C_8)$	118.1 (2)		
$\theta(C_4N_3C_8)$	125.0 (3)		

[a] Bond distances in Å. Bond angles in deg.

(11) Walker, N.; Stuart, D. *Acta Crystallogr., Sect A: Found. Crystallogr.* **1983**, *A39*, 158.
(12) Calabrese, J. C., Ph.D Thesis, University of Wisconsin, 1971.
(13) Main, P.; Lessinger, L.; Woolfson, M. M.; Germain, G.; Declarq, J. P. MULTAN, York, England, and Louvain-la-Neuve, Belgium, 1978.
(14) *International Tables for X-ray Crystallography*; Kynoch Press: Birmingham, England, 1974; Vol. IV.
(15) (a) Dupuis, M.; Rys, J.; King, H. F. *J. Chem. Phys.* **1976**, *65*, 111. (b) King, H. F.; Dupuis, M.; Rys, J. *National Resource for Computer Chemistry Software Catalog, Program* QH02 (HONDO), 1980; Vol. 1.
(16) Dunning, T. H., Jr.; Hay, P. J. In *Methods of Electronic Structure Theory*; Schaefer, H. F., III., Ed.; Plenum Press: New York, 1977; p 1.
(17) Pulay, P. In *Applications of Electronic Structure Theory*; Schaefer, H. F., III., Ed.; Plenum Press: New York, 1977; p 153.
(18) GRADSCF is an ab initio gradient program system designed and written by A. Komornicki at Polyatomics Research and supported on grants through NASA-Ames Research Center.
(19) McLean, A. D.; Chandler, G. S. *J. Chem. Phys.* **1980**, *72*, 5639.
(20) Dunning, T. H., Jr. *J. Chem. Phys.* **1970**, *53*, 2823.

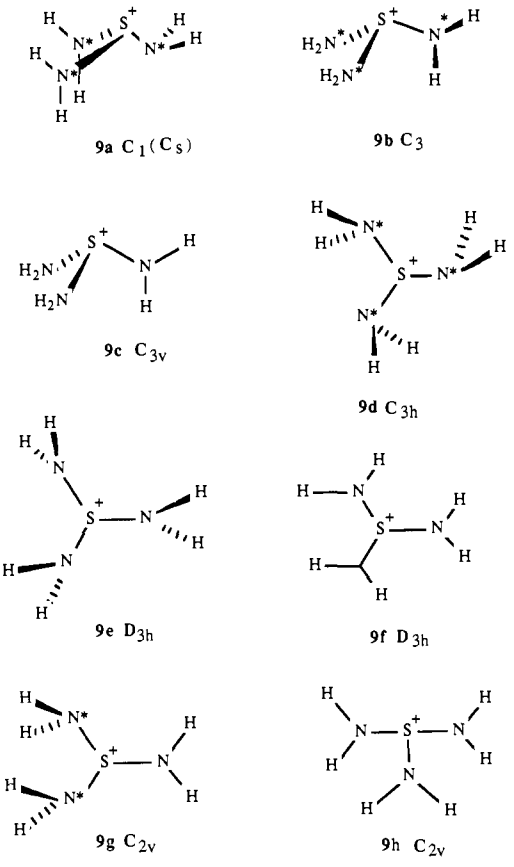

Figure 1. Conformations and point groups for planar and pyramidal $S(NH_2)_3^+$. Starred nitrogens are pyramidal.

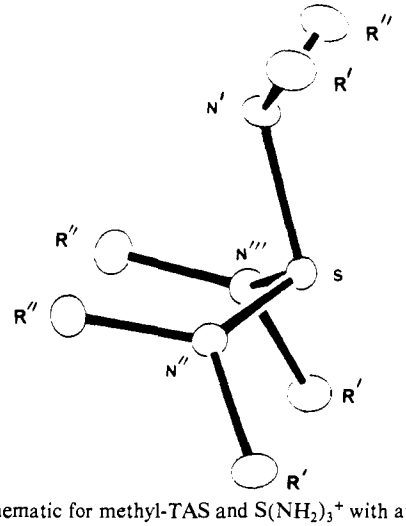

Figure 2. Schematic for methyl-TAS and $S(NH_2)_3^+$ with atomic labels.

a planar S^+. In **9e** and **9f**, both the sulfur and the nitrogens are trigonal planar. In **9e**, the hydrogen atoms are above and below the plane containing the S and N atoms while for **9f** the hydrogen atoms are in the S–N plane. Structure **9d** is derived from **9e** by allowing the nitrogens to become pyramidal. Structure **9g** has sulfur and one nitrogen planar with the hydrogen atoms on the planar nitrogen in the S–N plane. The other two nitrogens are pyramidal (structure **9g** is formed by rotation about one S–N bond in **9d**). Structure **9h** is formed by allowing **9f** to relax its symmetry to C_{2v} so that there are two axial planar NH_2 groups and one equatorial planar NH_2 group.

Results and Discussion

Crystal Structure. The bond distances and angles for the heavy atoms in the methyl-TAS cation are given in Table II (see Figure 2 for numbering convention) for the salts **1** through **6**. Since there

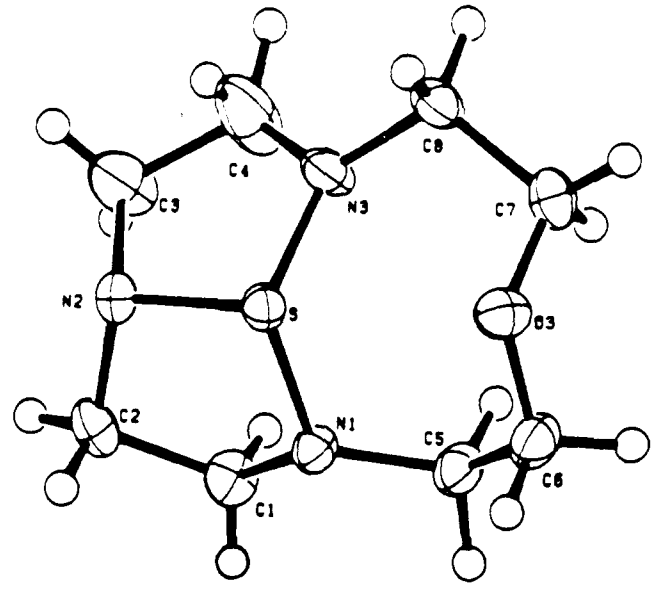

Figure 3. X-ray crystal structure of **7** with atomic labels.

Table IV. Average Bond Distances and Angles for Methyl-TAS, Experimental, and $S(NH_2)_3^+$, Calculated[a]

parameter	methyl-TAS (raw ave)	methyl-TAS (final ave)	**9**	**9** (ave)
S–N′	1.689	1.689	1.661	1.661
S–N″	1.617	1.615	1.618	1.618
S–N″	1.613		1.617	
N′–R′	1.483	1.481	1.011	1.011
N′–R″	1.479		1.011	
N″–R″	1.474	1.470	1.010	1.010
N″–R′	1.468	1.466	1.008	1.008
N″–R″	1.467		1.010	
N″–R′	1.464		1.008	
θ(SN′R′)	111.3	111.5	110.9	110.9
θ(SN′R″)	111.7		110.9	
θ(R′N′R″)	110.7	110.7	110.8	110.8
θ(SN″R′)	114.2	115.0	115.7	115.8
θ(SN″R″)	123.3	123.6	118.8	118.8
θ(R′N″R″)	115.2	115.5	116.0	116.0
θ(SN″R′)	115.9		115.9	
θ(SN″R″)	123.9		118.9	
θ(R′N″R″)	115.7		115.9	
θ(N′SN″)	99.2	99.2	97.2	97.2
θ(N′SN″)	99.3		97.3	
θ(N″SN″)	115.4	115.4	114.2	114.2

[a] All bond distances in Å. All bond angles in deg.

are two crystallographically independent methyl-TAS cations for the salts **1** and **5**, both are given in Table II. The structural parameters for **7** are given in Table III following the atomic labels given in Figure 3. The average values for the parameters for methyl-TAS are given in Table IV together with the calculated values for $S(NH_2)_3^+$. The atomic coordinates and temperature parameters are given in supplementary tables together with the structure factors for the previously unpublished structures.

The structural parameters for the methyl-TAS cations from **1–6** are remarkably similar and are essentially independent of the structure of the counterion. (The largest deviations are found for **3** where the interaction between the anion and cation is quite strong.)[21] We use the average values in the following discussion. The structure is characterized by a single long S–N bond (to atom N′), r(S–N′) = 1.689 Å, and two shorter S–N bonds (to atoms N″), r(S–N″) = 1.615 Å, that are essentially equal. Nitrogen

(21) Examination of the crystal-packing diagrams shows that the closest interactions for these salts all involve those between cations and anions and that these interactions occur, in general, at reasonably long distances. For example, for **3**, the closest interactions between the bifluoride F's and S^+ are ~3.5 Å; in **4**, the closest interaction between S^+ and CF_3O^- is an S–O distance of ~3.5 Å.

Table V. Geometry Parameters for 9 for Conformational Analysis[a]

parameter	9b	9c	9d	9e	9f	9g	9h
r(S–N)	1.637	1.613	1.630	1.602	1.777	1.602, 1.672 (r)	1.681 (ax), 1.596 (eq)
r(NH)	1.010	1.004	1.008	1.004	1.016	1.001, 1.007 (r)	1.013 (ax), 1.001
r(NH′)	1.011	1.005					1.010
θ(NSN)	105.5	106.4	120.0	120.0	120.0	130.4, 114.8 (×2)	179.5, 89.7 (×2)
θ(HNH)	111.2	118.6	114.5	114.5	111.6	118.1, 125.2 (r)	111.9, 117.8 (eq)
θ(SNH)	111.7	117.6	114.7	114.7	124.2	118.5, 117.4 (r)	111.9, 121.1 (eq)
θ(SNH′)	116.3	123.8					136.2
ΔE (kcal/mol)[b]	2.8	7.7	46.0	49.0	192.9	68.6	85.5

[a] Bond distances in Å. Bond angles in deg. [b] Energy difference between **9a** and **9x** where x = b–h.

atoms N″ make an angle with sulfur, θ(N″SN″), of 115.4° while the other two bond angles θ(N′SN″) are much smaller, 99.2°. The ion thus has approximate C_S symmetry with two equivalent nitrogen atoms.

The bond distances in the methyl-TAS cation can be compared with the S–N bond distance found in $((CH_3)_2N)_2S$, r(S–N) = 1.686 Å,[22] which can be taken as a normal S–N single bond. The S–N bond distances in $((CH_3)_2N)_2SO_2$[23] and in **16**[24] are shorter,

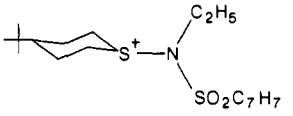

16

r(S–N) = 1.623 (5) and 1.644 (5) Å, respectively. In both cases back-bonding from the nitrogen lone pair to a virtual orbital on sulfur has been invoked to explain the short bond, i.e., a short S–N bond implies some component of multiple-bond character. Other examples[25] of this variation in S–N bond lengths can also be found.

The bond angles at tricoordinate S^+ tend to be near 100°. For example, the HSH bond angles in SH_3^+ are 94.5°[26] (SCF-CI), while the CSC angle in $(CH_3)_2SO$ is 96.6° with θ(CSO) = 106.5°.[27] Thus the N′SN″ bond angles are "normal" for tricoordinate sulfur while the N″SN″ angle is quite large, consistent with the multiply bonded S–N″ bonds. The bond angles at the nitrogen atoms are also consistent with this result. The average sum of bond angles at N′ is only 333.7°, and N′ is clearly pyramidal. The nitrogens, N″, are almost planar with an average bond angle sum of 354.1°. The C′N″S bond angle is significantly greater than θ(C′N″S). This probably occurs because of steric repulsions between the methyl groups on the more hindered back side of the sulfur pyramid. The $(CH_3)_2N''$ group rocks up into the vacant front side of the sulfur pyramid to alleviate this interaction.

The orientation of the methyl groups about the nitrogens is consistent with these arguments (see A). The unique nitrogen

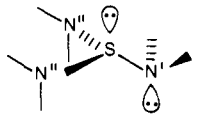

A

is oriented with its substituents staggered such that the lone pair on N′ is anti to the lone pair on S. This is consistent with a lack of multiple bonding at this nitrogen. For the other two nitrogens, the methyl groups are rotated by 90° so that the C–N″ bonds approximately eclipse the S lone pair. The lone pair on nitrogen N″ is approximately "perpendicular" to the lone pair on sulfur and thus available for interaction with d orbitals on sulfur to form multiple bonds.

Calculations. Ground State. The calculated structure for $S(NH_2)_3^+$ has approximate C_s symmetry and is in excellent agreement with the average experimental structural parameters for methyl-TAS. The S–N′ bond is ~0.03 Å shorter in $S(NH_2)_3^+$ than in methyl-TAS while the two S–N″ distances are slightly longer. Thus $S(NH_2)_3^+$ probably has a little less multiple bonding in the S–N″ bond than found in methyl-TAS. This could arise because of different steric effects in the two compounds. The angles at S are similar in both molecules with the N′SN″ angles being 2° smaller in $S(NH_2)_3^+$ and the N″SN″ angle being 1.2° smaller. The HN′S and HN′H angles are essentially the same as the CN′S and CN′C bond angles at the unique nitrogen. At the equivalent nitrogens, N″, the H′N″S and C′N″S angles and the H′N″H″ and C′N″C″ angles are quite similar. The H″N″S angle in **9a** is significantly smaller than the C″N″S angle in methyl-TAS. Thus the N″ nitrogens exhibit greater pyramidality (350.6°) in $S(NH_2)_3^+$ than in methyl-TAS. This difference in bond angles could arise from the different steric bulk of H and CH_3. The orientations of the $N'H_2$ and $N''H_2$ groups are the same as those found in methyl-TAS. Thus the calculated structure for the unsubstituted ion reflects all of the important features of the X-ray results.

Conformational Properties of $S(NH_2)_3^+$. We have studied a number of other conformations in order to examine the inversion barrier in $S(NH_2)_3^+$ and to study rotation about the S–N bonds. The other structures are all higher in energy than the optimum structure, and the parameters are given in Table V. Structure **9b** is only 2.8 kcal/mol higher in energy than the ground state, structure **9a**. Conceptually, **9b** is derived from **9a** by rotation about the S–N′ bond, allowing all the nitrogens to be pyramidal and then enforcing C_3 symmetry. The value for r(S–N) of 1.637 Å in **9b** is just about the average value of 1.633 Å found for **9a**. The NSN bond angles open up from those in H_3S^+ [θ(HSH) = 96.5° (SCF)][26] and are more like θ(CSO) in $(CH_3)_2SO$.[27] Forcing the nitrogens to be planar (**9c**) causes the energy to increase to 7.7 kcal/mol above that of **9a**. The S–N bond distance shortens as expected for bonding to a planar nitrogen, and θ(NSN) increases by about 1°. The energy difference between **9b** and **9c** of 4.9 kcal/mol corresponds to the inversion of the three nitrogens in $S(NH_2)_3^+$. The average value of 1.6 kcal/mol for inversion at each N is between that expected for SiH_3NH_2 (0.3 kcal/mol)[28] which is almost planar and that of NH_3 (5.8 kcal/mol)[29] or CH_3NH_2 (4.8 kcal/mol).[30] However, it is clear that if the sulfur remains pyramidal, the S–N rotation barrier is low as are the inversion barriers at N.

The low inversion barriers at N and low rotation barriers about the C–N bond described above for a pyramidal S^+ are consistent with the experimental result that the CH_3 groups in methyl-TAS are all equivalent on the NMR time scale at temperatures as low as −90 °C. Although the motion for exchanging CH_3 groups is complicated—rotation about the S–N bond, planarization of N, S–N bond rotation, and pyramidalization of N—these motions can take place rapidly due to the low barriers.

(22) Hargittai, I.; Hargittai, M.; Hernadi, J. *Magyar. Kem. Fol.* **1970**, *76*, 63.
(23) Jordan, T.; Warren-Smith, H.; Lohr, L. L., Jr.; Lipscomb, W. N. *J. Am. Chem. Soc.* **1963**, *85*, 846.
(24) Cook, R. E.; Glick, M. D.; Rigau, J. J.; Johnson, C. R. *J. Am. Chem. Soc.* **1971**, *93*, 924.
(25) Kresze, G. *Organic Sulfur Chemistry*; Stirling, C. J. M., Ed.; Butterworth: 1975; p 65.
(26) Dixon, D. A.; Marynick, D. S. *J. Chem. Phys.* **1979**, *71*, 2860.
(27) Feder, W.; Dreizler, H.; Rudolph, H. D.; Typke, V. *Z. Naturforsch., A: Astrophys., Phys., Phys. Chem.* **1969**, *24A*, 266.
(28) Dixon, D. A. unpublished results.
(29) Swalen, J. D.; Ibers, J. A. *J. Chem. Phys.* **1962**, *36*, 1914.
(30) (a) Tsuboi, M.; Hirakawa, A. Y.; Tamagake, K. *J. Mol. Spectrosc.* **1967**, *22*, 272. (b) Eades, R. A.; Weil, D. A.; Dixon, D. A.; Douglass, C. H., Jr. *J. Phys. Chem.* **1981**, *85*, 976.

There has been a significant amount of work on the inversion barriers for trivalent sulfur.[31] Extensive SCF-CI calculations with large basis sets give an inversion barrier of 32.2 (31.6-SCF) kcal/mol for SH_3^+.[26] We have calculated the inversion barrier for $S(NH_2)_3^+$ in order to examine the effect of substituting NH_2 for H and to eliminate the inversion process at sulfur as being the motion that makes the CH_3 groups equivalent on the NMR time scale.

The likely orientations for the NH_2 groups which are lowest in energy are shown, **9d** or **9e**, where the nitrogen lone pairs are perpendicular to the sulfur lone pair. The structures for **9d** and **9e** are very similar to **9b** and **9c**, respectively, except that the S^+ is pyramidal for the latter two. The value for r(S–N) shortens slightly in going from pyramidal to planar sulfur; the difference between **9b** and **9d** is 0.007 Å while that between **9c** and **9e** is 0.011 Å. The energy difference between **9d** and **9e** is 3.0 kcal/mol as compared to the difference of 4.9 kcal/mol found between **9b** and **9c**.

The planar S^+ structures **9d** and **9e** are 46.0 and 49.0 kcal/mol, respectively, higher in energy than **9a**. Clearly inversion at S^+ is not a low-energy process leading to the interchange of CH_3 groups.

In order to examine the effect of substituting NH_2 for H at sulfur on the inversion barrier, it is more appropriate to examine ΔE(**9b–9d**) and ΔE(**9c–9e**) eliminating problems with conformational changes at nitrogen. The value for ΔE(**9b–9d**) is 43.2 kcal/mol while ΔE(**9c–9e**) is 41.3 kcal/mol. The inversion barrier thus increases by 10–12 kcal/mol when NH_2 is substituted for H. This example is of interest because the repulsive π interactions between the lone pairs on N and S are eliminated in the planar state and inductive effects should dominate. Simple arguments based on the inductive effect suggest that electron-withdrawing groups (e.g., NH_2) should destabilize the planar form because the energy required to form an sp^2 hybrid is increased. This type of behavior has been observed in comparisons[32,33] of the inversion barriers for AH_3 and AH_xF_y($x + y = 3$, A = Group V element) compounds with the added problem of π-electron repulsion in the planar form for the AH_xF_y compounds. For $y > 0$, these compounds tend to have extremely high barriers for a planar trigonal inversion.

If all of the nitrogen atoms are coplanar with the sulfur, there is a large repulsive interaction due to the presence of 8 electrons in four overlapping p orbitals. This corresponds to a very high

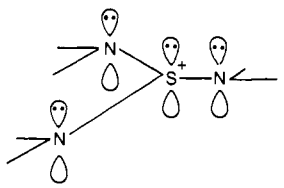

energy structure. Calculations on this geometry show that the HOMO is not in a p-orbital (a_2'') on S^+ but rather is in an in-plane orbital of a_1' symmetry with a significant "s" component. This HOMO symmetry switching has previously been observed for PF_3.[34] The S–N bonds become quite long, and the inversion barrier through this structure is 193 kcal/mol. A similar result is found for SF_3^+ with an inversion barrier of 154.2 kcal/mol through a trigonal planar structure.[33b]

It has recently been shown that compounds involving P, As, or Sb may invert through a planar T-shaped structure like **9h** rather than through a planar trigonal structure like **9f**. For example, the inversion barrier in PF_3 is lowered from 124.9 kcal/mol (D_{3h}) to 68.6 kcal/mol (C_{2v}), and for SF_3^+ the barrier decreases from 154.2 kcal/mol to 89.6 kcal/mol.[33] Structure **9h** is much lower in energy than structure **9f**, and if **9** would invert through a structure with all planar nitrogens, it would proceed via the T-shaped structure with an inversion barrier of 85.5 kcal/mol. The geometry of **9h** shows a short S–N equatorial bond and two long S–N axial bonds. This structural feature is found in other T-shaped transition states. The N_{ax}–S–N_{ax} bond angle is ~180°. The other geometric features are as expected.

We also optimized the structure **9g** starting from a T-shaped structure. Structure **9g** is obtained by rotating the two axial nitrogens in **9h** by 90°. However, for this case, the HOMO is a p out-of-plane orbital, and the structure optimizes to the expected trigonal planar structure. This structure is significantly higher in energy than that found for **9d** showing a large rotation barrier about an S–N bond in **9d** if the nitrogen becomes planar. The two unrotated nitrogens have short S–N bonds (like those in **9e**) while the S–N_r bond is quite long. This long bond is presumably due to electronic repulsions between the lone pairs on N and S^+. The NSN bond angle has opened up to 130.4° while the two NSN_r bond angles are ~115°. The rotated nitrogen N_r is rigorously planar, and the other two nitrogens are almost planar with a bond angle sum of 354.7° at each nitrogen.

Table VI. Calculated Vibrational Frequencies and Infrared Intensities for $S(NH_2)_3^+$

freq (cm^{-1})	freq scaled (cm^{-1})	intensity (km/mol)	assignment
299	269	0.9	torsion S–N′
317	285	41.3	torsion N–H″ (sym)
352	317	17.4	bend N″–S–N″ (sym)
417	375	8.4	inversion at S
478	430	194.1	inversion at N″ (asym)
503	453	19.9	torsion S–N″ (asym)
547	492	219.4	bend N″–S–N″ (asym)
590	531	175.8	inversion at N″ (sym)
840	756	129.2	stretch S–N′
927	834	65.7	inversion at N′
989	890	124.3	stretch S–N″ (sym)
1001	901	87.9	stretch S–N″ (asym)
1103	993	0.2	bend H–N″–H (sym)
1209	1088	34.0	bend H–N″–H (sym)
1259	1133	11.0	bend H–N′–H (sym)
1693	1524	50.4	bend H–N″–H (asym)
1695	1526	138.9	bend H–N″–H (asym)
1724	1552	14.5	bend H–N′–H (asym)
3703	3333	164.2	stretch N′–H (sym)
3707	3336	114.3	stretch N″–H (sym)
3712	3341	99.2	stretch N″–H (sym)
3811	3430	121.8	stretch N′–H (asym)
3843	3459	92.2	stretch N″–H (asym)
3846	3461	232.4	stretch N″–H (asym)

Calculated Vibrational Frequencies. The vibrational frequencies and infrared intensities for $S(NH_2)_3^+$ were determined analytically and are given in Table VI. Frequencies scaled by 10% have also been given in order to account approximately for correlation effects and anharmonic corrections, and the scaled frequencies are used in the following discussion. The lack of any imaginary frequencies confirms our determination of the structure of **9a** as being a minimum on the potential energy surface. The frequencies are assigned by examination of the eigenvectors in terms of a set of internal coordinates. The assignments given below are approximate because of the large couplings between various motions.

The N–H stretches occur in the region of 3330–3475 cm^{-1}. The N–H stretching frequencies at N′ are lower than those at N″. This is consistent with the planarity at N″. The asymmetric groupings occur at higher frequencies than the symmetric groupings. These stretches are all predicted to be reasonably intense. The asymmetric HNH bends are found near 1525–1550 cm^{-1} with the bend at N′ being higher than those at the N″'s. The symmetric HNH bends are found at lower frequencies, 990–1130 cm^{-1}, with the bend at N′ again occurring at the highest frequency. We note that the symmetric grouping of these HN″H bends is at higher frequency (1088 cm^{-1}) than the asymmetric grouping

(31) Allen, L. C.; Rauk, A.; Mislow, K. *Angew. Chem. Int. Ed. Engl.* **1970**, *9*, 400.
(32) (a) Schmeidekamp, A.; Skaarup, S.; Pulay, P.; Boggs, J. E. *J. Chem. Phys.* **1977**, *66*, 5769. (b) Boggs, J. E.; Seida, D. *J. Chem. Phys.* **1981**, *85*, 3645.
(33) (a) Dixon, D. A.; Arduengo, A. J., III.; Fukunaga, T. *J. Am. Chem. Soc.* **1986**, *108*, 2461. (b) Dixon, D. A.; Arduengo, A. J., III *J. Chem. Soc., Chem. Commun.*, submitted.
(34) (a) Marynick, D. S. *J. Chem. Phys.* **1980**, *73*, 3939. (b) Marynick, D. S.; Rosen, D. C.; Liebman, J. F. *J. Mol. Struct.* **1983**, *94*, 47.

Table VII. Mulliken Charges for $S(NH_2)_3^+$ [a]

atom	charge	atom	charge
S	+0.92	H	+0.26
N′	−0.50	H′	+0.28
N″	−0.52	H″	+0.27
N″	−0.52	H′	+0.28
H	+0.26	H″	+0.27

[a] All charges in electrons.

(993 cm^{-1}). There is very little intensity in this latter band. The S–N stretches are mixed to some extent with the inversion barrier at N′. As expected the S–N″ stretches are at higher frequencies, near 900 cm^{-1}, than the S–N′ stretch which is at 756 cm^{-1}. The S–N stretching frequencies are all reasonably intense. The $N'H_2$ wag (inversion at N′) is predicted to be at 834 cm^{-1}. For comparison, the inversion frequency in NH_3 is at 950 cm^{-1} while the NH_2 wag in CH_3NH_2 is at 780 cm^{-1}.[35] The $N'H_2$ wag has a moderate intensity of 66 km/mol. As expected from the near planarity at N″, the $N''H_2$ wags are much lower with the symmetric grouping at 531 cm^{-1} and the asymmetric grouping at 430 cm^{-1}. Both transitions are predicted to be very intense, more so than the inversion at N′.

The remaining frequencies involve the N–S–N bends including the inversion at S^+ and the torsions about the S–N bonds. There are significant couplings between many of the modes for these lower frequencies. As expected, from the multiple bond character in the S–N″ bonds, the torsion frequencies for rotation about these bonds are higher than those for rotation about the S–N′ bond. The asymmetric grouping for the S–N″ torsions is at 453 cm^{-1} while the symmetric grouping is at 285 cm^{-1}. The torsional frequency for th S–N′ bond is 269 cm^{-1}. The S–N″ torsional frequencies are much more intense than the frequency for S–N′ torsion which is extremely weak. For comparison, the torsion frequency in CH_3NH_2 is 268 cm^{-1}.[35] Inversion at S^+ is predicted at 375 cm^{-1} and is much less intense than the inversions at nitrogen. This is consistent with the much higher inversion barrier at S^+ than at N. The N″SN″ bends are at 492 cm^{-1} (asymmetric) and at 317 cm^{-1} (symmetric) with the asymmetric bend having a much higher intensity than the symmetric bend.

Electronic Structure of $S(NH_2)_3^+$. The Mulliken charges for $S(NH_2)_3^+$ are given in Table VII. The sulfur is quite positive with +0.92e and the remaining positive charge on the NH_2 groups. The nitrogens are quite negative with the unique nitrogen slightly less negative (0.02e) than the other two nitrogens. The amino group charges (addition of the charges of the bonded hydrogens to the nitrogen charge) are opposite with the unique amino group being slightly more negative (a difference of 0.03e) than the two other amino groups.[36]

The three highest lying MO's are predominantly of lone pair character. The HOMO at 16.97 eV has 1.03e on N′ and 0.65e on S. The next two orbitals at 17.27 eV and at 19.04 eV are predominantly composed of the two lone pairs on the N″'s. Thus the most available electrons in this system are on the nitrogens which is consistent with the very high positive charge on the sulfur. This is also consistent with the higher inversion barrier at S^+ when NH_2 is substituted for H since the character of the HOMO has to change more drastically on inverting $S(NH_2)_3^+$ than for inverting H_3S^+.

Crystal Structure for 7. The structure for **7** shows clear deviations from the structures of methyl-TAS and $S(NH_2)_3^+$ (see Table III and Figure 3). The deviations may be occurring because the nitrogen atoms are bridgeheads in this tricyclic compound. The structure for **7** does have one large NSN bond angle of 113° and two smaller NSN angles of 95° as expected from the previous structures. However, the S–N bond distances are all longer than would be expected, ranging from 1.644 to 1.704 Å. The structure does have the longest S–N bond opposite the largest NSN bond angle, and this nitrogen is the "unique" nitrogen in terms of a methyl-TAS-like structure. This nitrogen, N_2, is clearly pyramidal (sum of angles = 331°) although $\theta(CN_2C)$ is quite large, 115°. The nitrogen with the shortest S–N bond, N_3, is essentially planar (358°). The CN_3C angle is quite large, 125°. The S–N_3 bond is somewhat longer than might be expected based on our methyl-TAS results because of the strain due to the nitrogen being a bridgehead for a bicyclic system involving a five-membered ring and an eight-membered ring. The remaining nitrogen, N_1, is clearly pyramidal (343.5°), and the S–N bond is essentially that of a single bond. This nitrogen is more strained than the other nitrogen in a similar position, N_3.

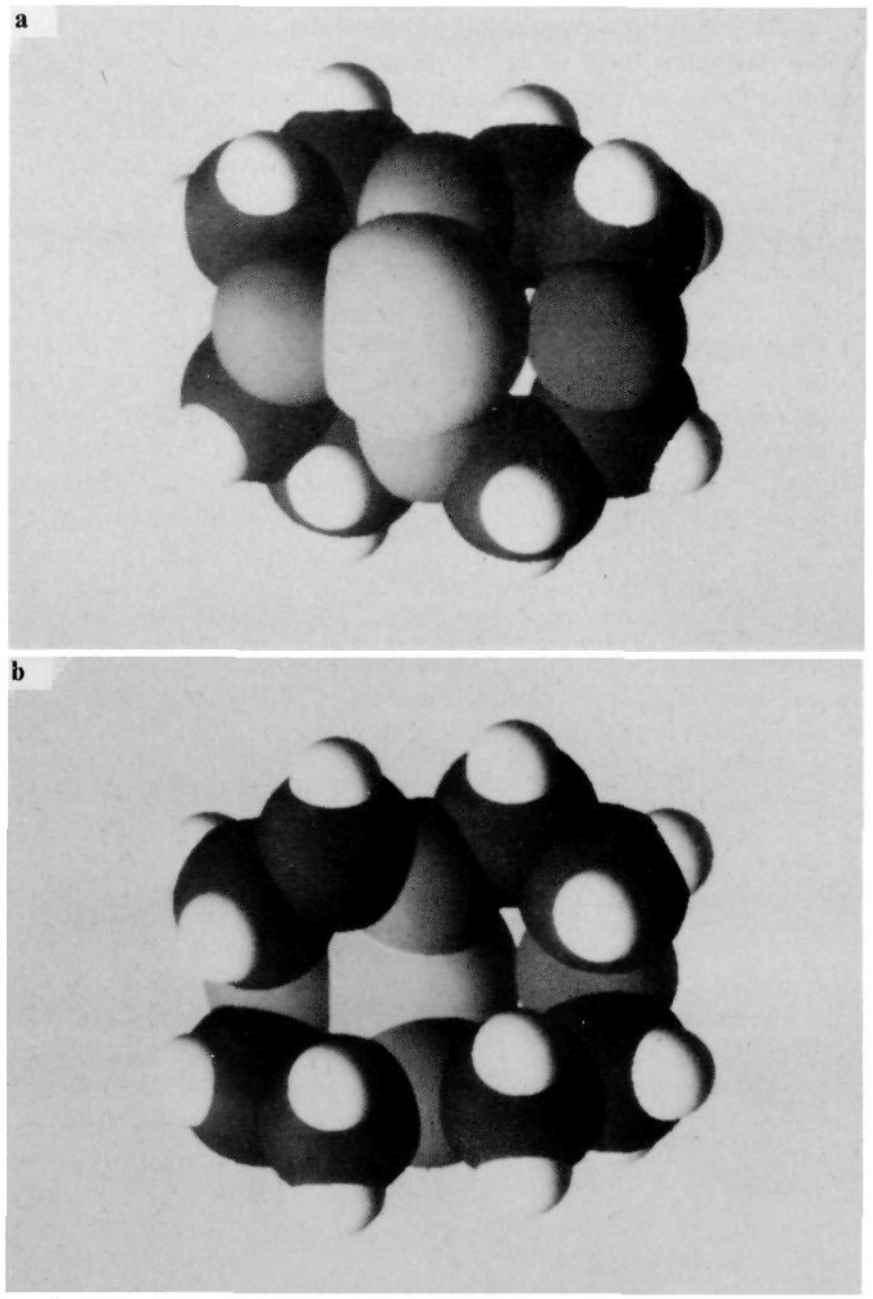

Figure 4. Two molecular graphics views of TAS derivative **7**. (a) Top view of **7**. N_3 is at the top, N_1 is at the bottom, and N_2 is at the left. (b) Bottom view of **7** obtained by rotating about the horizontal axis in (a) by 180°. N_1 is at the top, and N_3 is at the bottom.

Two different views of **7** from molecular graphics are given in Figure 4. Clearly the conformations of the two five-membered rings are different, and the eight-membered ring is not symmetric across the N_2–S–O plane. The more planar nitrogen N_3 has the CH_2 groups bonded to it tilted more to the concave side of the S^+ than are those bonded to N_1. The N_3 side of the ion has more steric bulk on the concave side while the N_1 side has the CH_2 groups pushed more toward the open lone pair side. Thus the two nitrogens, N_1 and N_3, are in different environments and are not equivalent. By constraining N_2 at a bridgehead of a bicyclo[3.3.0]octane ring system, its lone pair is forced to be approximately syn to the lone pair on S^+ rather than anti as found in TAS^+. The S–N_2 bond is thus slightly elongated. Nitrogens N_3 and N_1 have their lone pairs at angles significantly greater than 0° to the sulfur lone pair, but they are not as close to being pependicular as found in methyl-TAS, and so less back-bonding from the nitrogen lone pairs to the virtual orbital on sulfur is

(35) Shimanochi, T. *Tables of Molecular Vibrational Frequencies. Consolidated Volume I*; NSRDS-NBS 39, National Bureau of Standards, U.S. Government Printing Office, Washington, DC, 1972.

(36) The charge differences are very small, and one should not give too much meaning to the differences. We do note that the group charges are consistent with donation from the two equivalent amino groups to the sulfur.

present. This is consistent with the longer S–N bonds to these two nitrogens.

One of the most striking features in **7** is the short S--O "nonbonded" distance of 2.55 Å. Although this distance is clearly much longer than a nominal S–O bond distance of 1.70 Å (sum of covalent radii), it is clearly much shorter than the sum of the van der Waals radii of (3.25 Å).[37] There is, then, a reasonably strong interaction between the S^+ and the O, probably an electrostatic polarization of the oxygen lone pairs by the cationic sulfur. Since the S–N bonds do not have significant multiple-bond character, the lone pairs on oxygen can also interact with the vacant d orbitals on the S^+ further strengthening the S–O interaction. It is probably this S–O interaction that is strongly perturbing the conformation of the eight-membered ring and perhaps the conformations at the nitrogens. The short S--O distance is only 0.20 Å longer than the strong S–O interaction in **17**[38] and is reminiscent of the bonding observed by Verkade and coworkers in compounds like **18**.[39] A similar long S–O bond is found[40] in the tetracoordinated sulfur system **19** where the S–O bond to the carboxylate ligand is 2.25 Å, and the other S–O bond is 1.66 Å. The S–C bonds are of normal length between 1.75 and 1.80 Å.

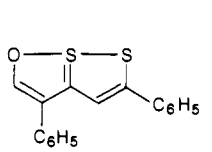

17

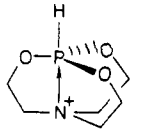

18

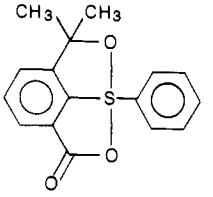

19

Registry No. 1, 105121-46-8; **2**, 105121-47-9; **3**, 85248-37-9; **4**, 96898-10-1; **5**, 79218-01-2; **6**, 91514-28-2; **8**, 105121-50-4; **10**, 91454-72-7; **11**, 53835-21-5; **12**, 105121-48-0; **15**, 70091-69-9; HF_2^-, 18130-74-0; $Me_3SiF_2^-$, 51202-29-0; diphenyldichlorosilane, 80-10-4; chlorotrimethylsilane, 75-77-4; tris(dimethylamino)sulfonium trimethyldifluorosiliconate, 59218-87-0.

Supplementary Material Available: Positional parameters, temperature factors, bond distances and angles, and labeled structures (27 pages); structure factor tables (14 pages). Ordering information is given on any current masthead page.

(37) Atkins, P. W. *Physical Chemistry*, 2nd ed.; W. H. Freeman & Company: San Francisco, CA, 1982, p 751, 756.
(38) Hordvik, A.; Sletten, E.; Sletten, J. *Acta. Chem. Scand.* **1969**, *23*, 1377.
(39) (a) Clardy, J. C.; Milbrath, D. S.; Springer, J. P.; Verkade, J. G. *J. Am. Chem. Soc.* **1976**, *99*, 623. (b) Carpenter, L. E., II.; Verkade, J. G. *J. Am. Chem. Soc.* **1985**, *107*, 7084.
(40) Lam, W. Y.; Duesler, E. N.; Martin, J. C. *J. Am. Chem. Soc.* **1981**, *103*, 127.

Chemometrics of the Solvent Basicity: Multivariate Analysis of the Basicity Scales Relevant to Nonprotogenic Solvents†

Pierre-Charles Maria,*‡ Jean-Francois Gal,‡ Jeanine de Franceschi,§ and Evelyne Fargin§

Contribution from the Laboratoire de Chimie Physique Organique, Université de Nice, 06034 Nice, France, and the Laboratoire de Prospective Réactionnelle et d'Analyse de l'Information, C.N.R.S., U.A. 126, Université d'Aix-Marseille III, Centre de Saint-Jérôme, 13397 Marseille, France. *Received June 17, 1986*

Abstract: The dimensionality of the basicity-dependent behavior in the condensed phase, of nonprotogenic organic molecules commonly used as solvents, is approached by a principal component analysis (PCA) of a set of basicity-dependent properties (BDPs) related to hydrogen bonding, proton transfer, and interactions with hard and soft Lewis acids, including the recent $-\Delta H°_{BF_3}$ basicity scale (*J. Phys. Chem.* **1985**, *89*, 1296–1304). By use of the Information theory, the original set of 10 thermodynamic and spectroscopic BDPs was reduced to the 5 most informative scales. This in turn allowed the inclusion of more solvents (22) representing the main classes of nonprotogenic organic media. The first two factors obtained by PCA account for about 95% of the total variance of the data. A physical significance is given to these factors by correlating them with intrinsic gas-phase affinities toward the proton and the potassium ion. A blend of electrostatic and charge-transfer or electron-delocalization characters is attributed to the first factor, which is colinear with proton affinity corrected for enhanced-polarizability effect. The correlation observed between the second factor and the potassium-ion affinity corresponds to an essentially electrostatic character. The third factor, of marginal importance, arises in part from the steric hindrance of complexation (front strain). The relationships between dissimilar BDPs are unraveled in terms of the differences between the sensitivities of the properties to the electrostatic, or long-range, and charge-transfer, or short-range, contributions to the adduct formation. These differences are visualized by a fan-shaped display of the angles $\theta = \tan^{-1}(S_2/S_1)$, associated with the ratio of sensitivities S_2 and S_1 to the second and third factors, respectively. Different BDPs, obtained from the same acid, show a regularity in their θ values, particularly the thermodynamic properties for which the electrostatic character increases in the order $\Delta S° < \Delta H° < \Delta G°$. An explanation is offered for the high charge-transfer character of $\Delta S°$ and the conversely high electrostatic character of $\Delta G°$. The Kamlet–Taft β parameter is shown to be a good descriptor of Gibbs free energies of hydrogen bonding.

The most popular word dealing with solvent effects is "polarity", a term not precisely defined, as noted by Reichardt.[1] If we consider, following him, that polarity represents the sum of all those molecular properties responsible for all the interaction forces between solvent and solute molecules, it seems rational that a model proposed to account for solvent effects will include *more*

† Presented in part at the Third International Euchem Conference on Correlation Analysis in Organic and Biological Chemistry, Louvain-La-Neuve, Belgium, July 15–18, 1985.
‡ Université de Nice.
§ Université d'Aix-Marseille III.

(1) Reichardt, C. *Solvent Effects in Organic Chemistry*; Verlag Chemie: Weinheim, 1979.

0002-7863/87/1509-0483$01.50/0